Meteorological influences on the surface hydrographic patterns of the North Aegean Sea*

OCEANOLOGIA, 53 (1), 2011.
pp. 57–80.

KEYWORDS
Water masses
Meteorological influences
Black Sea Water
Samothraki Anticyclone
North Aegean Sea

Georgios Sylaios

Department of Environmental Engineering,
Democritus University of Thrace,
GR–67100 Xanthi, Greece;

e-mail: gsylaios@env.duth.gr

Received 11 August 2010, revised 17 January 2011, accepted 18 January 2011.

Abstract

Hydrographic data from the North Aegean Sea were used to examine the summer variability of surface water masses during the period 1998–2001. Attention was placed on the surface hydrographic features of the area, such as the Black Sea Water (BSW) plume expansion, the frontal characteristics of the BSW with the Levantine Intermediate Water (LIW) and the variability of submesoscale hydrographic features (such as the Samothraki Anticyclone). Strong southerly wind stresses were found responsible for relaxing the horizontal density gradients across the BSW-LIW frontal zone and displacing this front to the north of Lemnos Island, thus suppressing the Samothraki Anticyclone towards the Thracian Sea continental shelf. Under northerly winds, the BSW-LIW front returns to its regular position (south of Lemnos Island), thus allowing the horizontal expansion of the Samothraki gyre up to the Athos Peninsula. Present results indicate the importance of medium-term wind stress effects on the generation of Samothraki Anticyclone suppression/expansion events.

* The data analysed in this study were collected during the MEDITS project, supported and funded under different contracts in the period 1998–2001 by EU DG Fisheries.

The complete text of the paper is available at http://www.iopan.gda.pl/oceanologia/

1. Introduction

The North Aegean Sea is a part of the Aegean Sea (Figure 1) experiencing complex bathymetric and hydrographic conditions (Lykousis et al. 2002). The bottom topography is characterized by a NE-SW oriented deep trough, separated by shallow sills and shelves, constituting the 'North Aegean Trough' (Poulos et al. 1997). Within this trough, three main depressions exist: the Lemnos Basin to the north-east (maximum depth 1470 m), the Athos Basin at the centre (maximum depth 1150 m) and the North Sporades Basin to the south-west (maximum depth 1500 m). A series of shallow sills separate these basins from the Skyros Basin to the south (maximum depth 1077 m), and from the Chios Basin to the west and south of Chios Island, with a maximum depth of 1200 m (Velaoras & Laskaratos 2005). The coastal morphology consists of a series of semi-enclosed gulfs, such as Alexandroupolis, Kavala and Strymonikos Gulfs to the north, Thermaikos Gulf to the north-west and North Evoikos Gulf to the west, where buoyancy inputs are supplied by moderate to high discharge rivers (i.e. the Rivers Evros, Nestos and Strymon along the northern coastline, and the Axios, Loudias, Aliakmon and Pinios in Thermaikos Gulf).

The most characteristic hydrographic feature of the area is the intrusion of low salinity (29–34), nutrient-rich Black Sea Water (BSW), which occupies the surface layer of the water column (20–40 m) and follows the

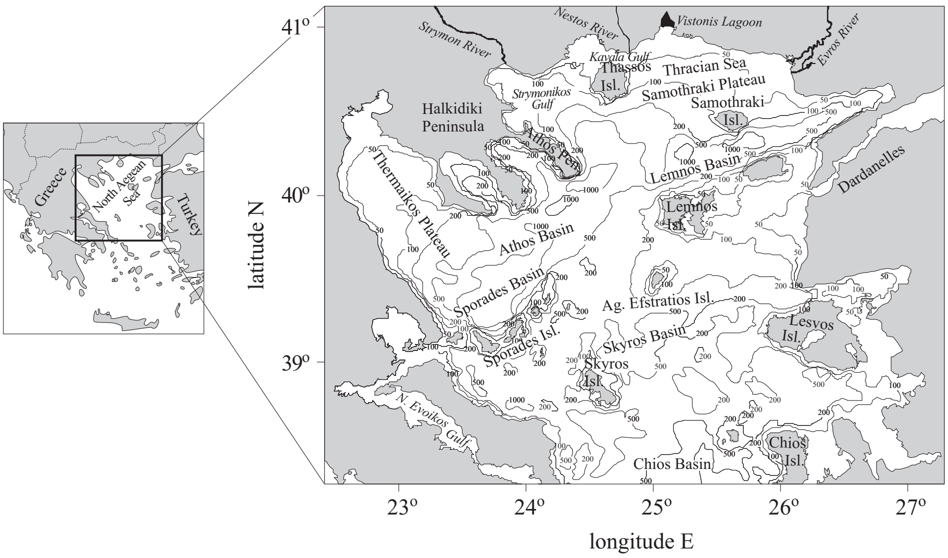

Figure 1. The North Aegean Sea and its main physiographic features

periphery of the cyclonic gyre (Ovchinnikov 1966), with deflecting branches over the Samothraki and Thermaikos Plateaus (Ünlüata et al. 1990, Latif et al. 1991). The North Aegean Sea appears to be mostly influenced by BSW during spring and summer (April to July), when the mean monthly outflow through the Dardanelles Straits reaches 15 000 m^3 s^{-1}, corresponding to the increased river runoff and precipitation over the Black Sea (Oguz & Sur 1989, Yüce 1995). The prevailing wind circulation controls the flow path of the BSW plume in the North Aegean Sea (Vlasenko et al. 1996). In the summer, after passing the Dardanelles, the main branch of the BSW flows south-westwards, under the influence of the annual northerly Etesian winds, with its core water appearing south of Lemnos Island (Poulos et al. 1997). In this region, a well-defined frontal zone is formed as a result of the interaction of the low salinity BSW and the more saline (38.5–39.0) Levantine Intermediate Water (LIW) originating from the Cretan Sea (Ivanov et al. 1989, Zodiatis et al. 1996). Moreover, a significant portion flows to the north of Lemnos Island (Theocharis & Georgopoulos 1993, Vlasenko et al. 1996, Zervakis & Georgopoulos 2002). In the winter, the BSW flows westwards, mostly along the northern coast of Lemnos, where it bifurcates primarily to the north-west and occasionally to the south-west, under the influence of north-easterly (bora-type) gales. This results in the accumulation of cold brackish water over the north-eastern part of the continental shelf, whereas warm and saline LIW appears in the south-eastern part (off Lesvos Island) (Zervakis & Georgopoulos 2002).

The vertical structure of the water column in the North Aegean Sea consists mainly of three layers: the low-salinity layer, with increased BSW presence at the surface; the warm and highly saline LIW, at depths from 50 to 400 m; and the very dense North Aegean Deep Water (NADW) at the bottom of each sub-basin (Lykousis et al. 2002). The BSW thickness depends on freshwater discharged through the Dardanelles and on wind shear, inducing vertical mixing with the underlying LIW layer (Zervakis et al. 2000). Through its course in the North Aegean Sea, BSW undergoes modification of its characteristics, gradually reaching a salinity of 38.0 in the region of the Sporades Islands (central and western Aegean Sea). Yüce (1995) considered the 38.7 isohaline as the lower limit of the BSW, resulting in the penetration of deeper BSW down to almost 100 m depth in the western part of the Aegean Sea.

Air-sea interactions and heat fluxes largely determine the convective movement of water masses in the area. The strong, cold and dry northerly winds, blowing over the Aegean Sea in summer (Lascaratos 1992), produce upwelling episodes of the Levantine-origin nutrient-depleted intermediate water along the western coasts of Lesvos and Lemnos Islands and along the Turkish coast. These events may produce a colder surface zone, with temperatures 2–3°C lower than in the northern and western parts of the Aegean Sea (Poulos et al. 1997). In the winter, heat losses induced by outbreaks of continental polar or arctic air masses, as well as evaporation, support the sinking of surface water across the shelf down to continental slope levels, where equilibrium may be reached. Such dense water formation processes have been reported to occur over the Samothraki and Lemnos plateaus by Gertman et al. (1990) and Theocharis & Georgopoulos (1993), enhanced by the presence of cyclonic eddies intruding and/or upwelling high salinity water in the area south of Thassos Island. Under these conditions, BSW may act as an insulator at the vicinity of its outflow to the North Aegean Sea, thus hindering dense water formation near the Lemnos Plateau (Zervakis et al. 2000). Therefore, the interannual variability in BSW thickness directly influences dense water formation along the Thracian Sea continental shelf (Zervakis et al. 2003).

Since the spreading of BSW is considered the most prominent feature of the upper North Aegean Sea, its dynamics and frontal characteristics, together with the meso- and small-scale cyclonic and anti-cyclonic patterns formed along its track, require special attention. These features show an important temporal variability as a result of the variable BSW outflows and changes in BSW characteristics, combined with the dynamic wind field prevailing in the area (Zodiatis 1994). Zervakis & Georgopoulos (2002) reported significant changes in the position of the BSW-LIW frontal zone on a seasonal basis. In terms of the eddy field, a permanent anticyclone of variable strength and dimensions has been revealed in the Thracian Sea, around Samothraki and possibly Imvros Islands (Theocharis & Georgopoulos 1993, Cordero 1999, Zervakis & Georgopoulos 2002). The gyre recirculates the BSW up to the Thracian Sea shelf, in the vicinity of the Evros river plume, inducing strong frontal conditions with the general cyclonic circulation, and aggregating and retaining the organic nitrogen and carbon-rich surface water (Zervakis & Georgopoulos 2002, Siokou-Frangou et al. 2002), thus favouring phytoplankton growth (Sempéré et al. 2002). Another cyclone of a semi-permanent nature covering the upper 200 m was observed in the Sporades Basin (Kontoyiannis et al. 2003) – it is supplied with higher salinity waters from the southern Aegean Sea. This feature co-exists with anticyclones of variable strength and size, dependent on the BSW inflow and Thermaikos Gulf freshwater outflows. Similarly, a cyclonic gyre exists at the entrance of the Thermaikos Gulf, transporting water inwards along the eastern coastline and outwards along the western coast of this gulf (Zervakis et al. 2005, Olson et al. 2007).

The current work presents collected hydrographic data and examines the surface distribution of water parameters (temperature, salinity, density and geopotential anomaly) during the summer periods of 1998–2001 with the aim of studying meteorological influences on the surface water patterns of the North Aegean Sea. In this work, special emphasis was placed on the BSW plume expansion, the BSW-LIW frontal characteristics and the variability of permanent and transient sub-basin gyre features.

2. Material and methods

The North Aegean Sea was visited during the summer periods in 1998–2001, on board the fishing trawler 'Evagelistria', for the conducting of experimental fishery research within the framework of the MEDITS (Mediterranean International Trawling Survey) programme. The area covered represents the whole North Aegean Sea and the northern part of the Central Aegean Sea, between 38–41°N and 22.5–26.3°E. Table 1 presents the starting and ending dates of each MEDITS summer cruise, together with the number of stations sampled per year. Standard hydrographic measurements were undertaken using a Seabird Electronics SBE 19 plus CTD. Sensor accuracy was 0.01°C for temperature and 0.01 mS cm^{-1} for conductivity. A total of 360 CTD casts were obtained during summers 1998–2001. The 1998 and 1999 cruises commenced from the Thracian Sea coastline (northern Aegean Sea border), followed a meridian transect through Lemnos, Lesvos and Chios Islands, and then moved north-westwards to the Sporades Islands, where the cruise ended. The 2000 and 2001 cruises followed a similar track, but extended to the northern Evoikos, Thermaikos and Strymonikos Gulfs (Figure 2). The 2000 and 2001 castings were limited to the first 200 m of the water column depth, to monitor surface dynamics and associate the collected data with the distribution of the ichthyofauna, which was sampled concurrently using a bongo net (0–50 m depth). The 1999 survey profiles were limited to 50 m depth.

Table 1. Summary characteristics of 1998–2001 MEDITS cruises

Year	Starting date	Ending date	Sampling stations
1998	17.06.1998	20.07.1998	106
1999	18.06.1999	26.07.1999	45
2000	21.06.2000	28.07.2000	106
2001	01.06.2001	13.07.2001	103

The raw data were filtered and processed according to the SBE software manual to derive water temperature and salinity as a 1-dbar

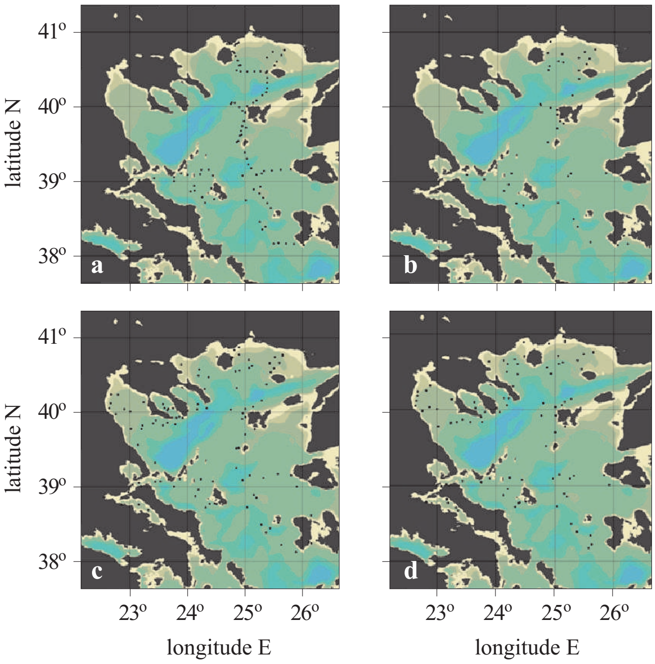

Figure 2. Sampling stations in the summer periods of 1998 (a), 1999 (b), 2000 (c), and 2001 (d)

bin average, together with potential temperature and density (σ_t-values). Standard routines (SeaMat library, available at http://woodshole.er.usgs.gov) were used to produce geopotential anomaly values (dynamic height in m multiplied by the acceleration due to gravity, expressed in J kg^{-1} or m^2 s^{-2}) at 5 dbars relative to 40 ($\Delta\Phi_{5/40}$) and 100 dbars ($\Delta\Phi_{5/100}$). Based on these values, geostrophic velocity vectors were then produced. Although a deeper reference level may be desirable (e.g. 200 dbars), previous studies have demonstrated the utility of the 40 and 100 m reference levels for capturing the effect of the BSW buoyancy input (Zervakis & Georgopoulos 2002). Processed data were imported to the ODV database (Ocean Data View, Schlitzer 2005) for further manipulation and export to relevant databases (e.g., WOCE, WOD, etc.). Horizontal maps of selected variables were produced using DIVA gridding software (Data Interpolating Variational Analysis), an algorithm that considers coastlines and bathymetry features for domain subdivision and performs better in the case of sparse and heterogeneous data coverage (signal-to-noise ratio = 40; quality limit = 1.5; excluding outliers). Meridional sections were produced for each parameter using VG gridding, utilizing data from the original sampling stations and not reconstructing them from the 3-D parameter field.

Meteorological data (air temperature, atmospheric pressure, wind speed and direction) for the period commencing fifteen days prior to the cruise start until the end of each annual cruise, were obtained from all the main airports of the broader North Aegean Sea area (Thessaloniki, Kavala, Alexandroupolis, Chios I., Lemnos I., Skyros I. and Istanbul). These data were combined with the surface wind vectors obtained from the NOAA 3-D atmospheric model, based on systematic satellite observations over the North Aegean Sea (http://www.arl.noaa.gov/ready/amet.html). Figure 3 presents a synoptic view of the surface wind vectors prevailing over the North Aegean Sea during each cruise period. The significant impact of the Etesians (north to north-easterly winds) during the 1998 to 2000 cruises is shown. Strong south to south-westerly winds, changing rapidly to northerlies, dominate during the 2001 sampling period.

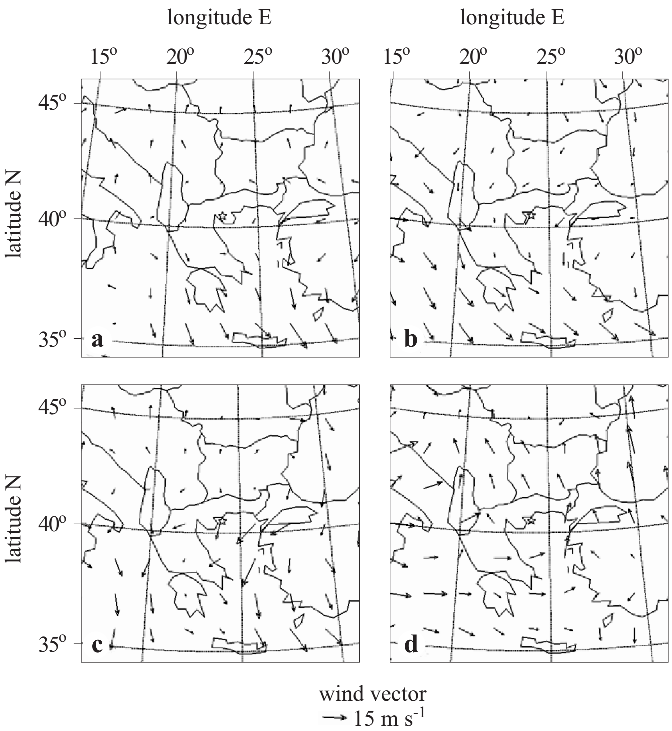

Figure 3. Mean wind vectors over the broader North Aegean Sea area in the sampling periods of summer 1998 (a), 1999 (b), 2000 (c), and 2001 (d)

3. Results

3.1. The 1998 cruise

The sea surface temperature displays a zonal distribution, with lower values (20–21°C) in the Thracian Sea and higher ones (23.2°C) in the Chios Basin (Figure 4a). This distinct north-to-south gradient is disrupted by the presence of cooler water (19–20°C) in the area south of Lemnos Island, corresponding to the BSW core. Relatively colder water occupies the surface layer along the eastern coastline of the North and Central Aegean Sea, with values 22–23°C near Lesvos and Chios Islands, compared to the warmer water (24.5°C) near the Sporades Islands. A similar zonal pattern is also exhibited by the surface salinity, with minimum values in an extended area south of Lemnos Island (28.7–29.3), occupied by the BSW. From this minimum, the surface salinity showed gradually increasing values of 33.0–34.5 towards the Thracian Sea and to the south-west towards the Sporades Basin (33.8–36.3) (Figure 4b). The very distinctive frontal zone separating the BSW and the LIW appears to be located in the vicinity of

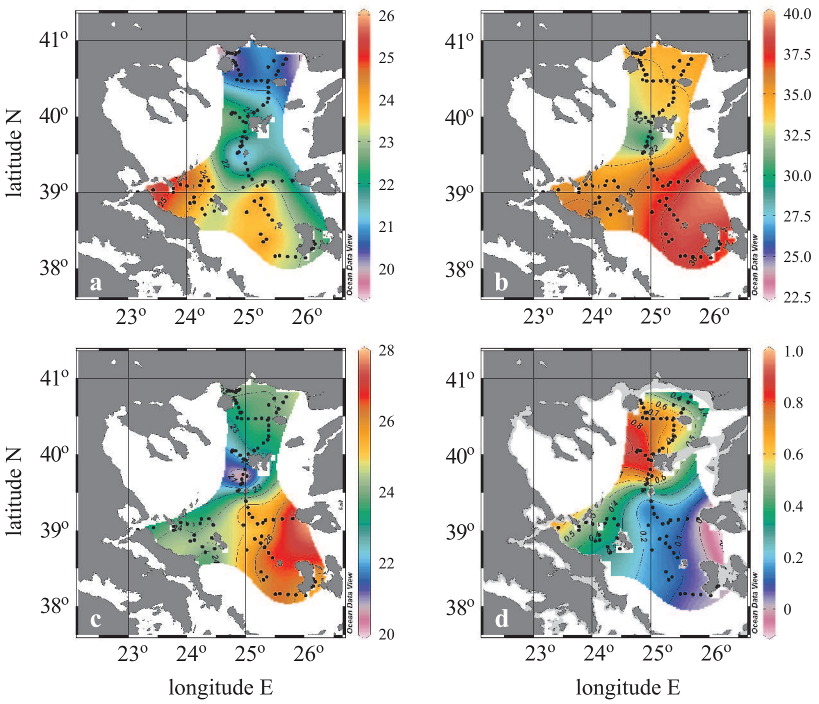

Figure 4. Horizontal distribution of water temperature (a), salinity (b), density σ_t (c) and geopotential anomaly ($\Delta\Phi_{0/40\,\mathrm{m}}$) (d) at the surface of the North Aegean Sea in summer 1998

Agios Efstratios Island. However, the 'closed-bull-eye' pattern in this area is mostly the result of the sparse and heterogeneous data coverage in this area, representing the exit of the BSW from the Dardanelles, rather than an existing hydrographic feature. The eastern coastline of the Aegean Sea is covered by water of Levantine origin, with typical high salinity values of 38.1 to 38.9. Figure 4c displays the horizontal σ_t-distribution, presenting patterns similar to those of salinity. The BSW is characterized by low density values (19.8–21.5); the Thracian Sea and the Sporades complex are almost homogeneous with moderate density levels of 23.8 to 24.2, while the Chios Basin shows elevated values (25.6–26.9). The horizontal geopotential anomaly distribution of $\Delta\Phi_{5/40}$ revealed the occurrence of the BSW-LIW frontal area, together with an anticyclonic gyre, moderate in strength ($\Delta\Phi_{5/40} = 0.90$ m^2 s^{-2}) and magnitude (40 km diameter), located to the north-west of Lemnos Island towards the Athos Peninsula (Figure 4d).

Figure 5 presents the temperature and salinity distribution along the meridian transect at 25°E to reveal differences in the water column structure along the North and Central Aegean Sea. Thermal and saline stratification prevail in the first 100 m of the Thracian Sea. The well-established thermocline occurring at 25 m depth in the Thracian Sea (15–16°C) sinks rapidly to 50 m depth near the Lemnos Plateau, diffusing gradually in the Skyros Basin, and further south in the Chios Basin, where almost homogeneous conditions (14–15°C) dominate between 50 and 200 m depth.

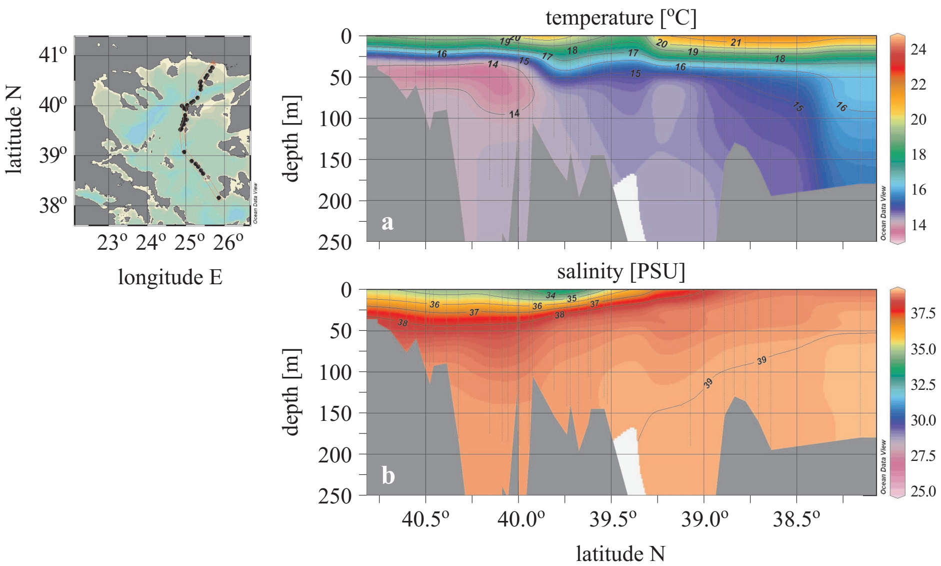

Figure 5. Distribution of water temperature (a) and salinity (b) along the 25°E meridian transect in summer 1998

Moreover, a cold water mass ($T = 13$–$14°$C) moving southwards from the Thracian Sea shelf (40–70 m depth), intruding the Lemnos Plateau water column at 100 m depth (Figure 5a), is the winter-originated BSW, which is trapped below the warmer summer BSW (Zervakis & Georgopoulos 2002). In the summer, the vertical expansion of the BSW gradually reaches 40 m depth at the Thracian Sea continental shelf, having isohalines sloping downwards at 1:2500 m or 0.01°. Well-mixed conditions prevail in the Skyros and Chios Basins covered with the highly saline LIW (Figure 5b).

3.2. The 1999 cruise

The BSW core ($T = 22$–$23°$C; $S = 32$–33; $\sigma_t = 21.2$–21.8) is detected along the southern coastline of Lemnos Island, with the BSW-LIW frontal zone located near Agios Efstratios Island. However, it is evident that the BSW-signal in the North Aegean is weaker compared to 1998, but with significant superficial expansion, especially towards the Thracian Sea and the western end of Lesvos Island. Thermal distribution shows the occurrence of cooler water (22–23°C) in the central and southern zones of the Chios and Skyros Basins and Lemnos Plateau, in contrast to the warmer Thracian Sea (23–24°C) (Figure 6a). Such a distribution relaxes the north-to-south temperature gradient, but induces a stronger east-to-west horizontal variability, due to the presence of warmer water (25–26°C) at the western end of Lesvos Island and in the Sporades complex, separated by cooler water in between (23°C). Surface salinity in the Thracian Sea and Lemnos Plateau is almost homogeneous, ranging between 31.3 and 33.2, exhibiting an abrupt change to 37.0 at the surface of the Skyros Basin, and further south-west towards the Sporades Islands (Figure 6b). The meridian surface density gradient, produced by a $\Delta\sigma_t$ difference of 5.6, dominates the

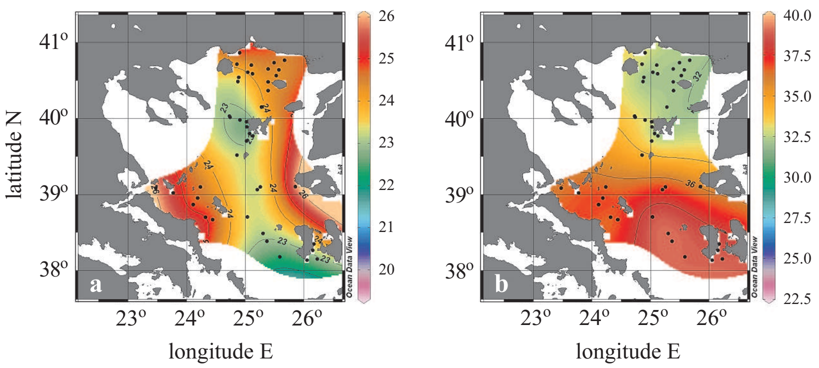

Figure 6. Horizontal distribution of water temperature (a) and salinity (b) at the surface of the North Aegean Sea in summer 1999

1999 distribution, with the evident entrapment of denser ($\sigma_t = 25.6$), highly saline ($S = 37.3$–37.5) surface water in the Sporades Basin.

3.3. The 2000 cruise

Strong thermal gradients in an east-to-west direction are displayed during this cruise, as a result of coastal upwelling under the influence of strong Etesian winds. Colder water (19.5–20.3°C) is observed in the Skyros Basin and the coastlines of Lesvos and Chios Islands (Figure 7a). In contrast, the water along the continental shelf of north-western Greece appears significantly warmer (24.2–25.7°C), especially in the Sporades and Athos Basins. The Thracian Sea and Lemnos Plateau exhibit almost uniform sea surface temperature (22.3–23.7°C) and salinity (34.1–34.8). The BSW-LIW convergence zone induces strong salinity gradients in the vicinity of Agios Efstratios Island (Figure 7b). The BSW core ($T = 22.5$°C; $S = 31.7$; $\sigma_t = 21.5$) is detected to the west of Lemnos Island. The northward branch of the BSW plume, consisting of gradually mixed water, appears defined by the 34-isohaline crossing Thassos Island. The south-western branch propagates

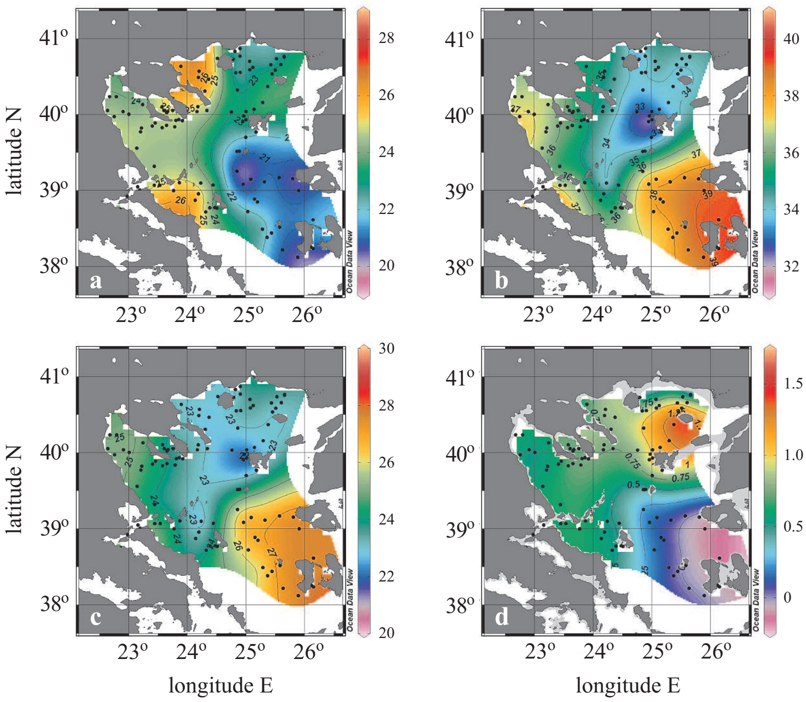

Figure 7. Horizontal distribution of water temperature (a), salinity (b), density σ_t (c) and geopotential anomaly ($\Delta\Phi_{0/40\,\mathrm{m}}$) (d) at the surface of the North Aegean Sea in summer 2000

in rapidly mixed surface patches, reaching the Sporades Basin with salinities between 33.0 and 36.5. Increased surface salinity values are recorded in the Thermaikos Gulf (36.6–37.2), due to the limited influence of river-induced inputs (Figure 7b). The highly saline LIW covers uniformly the surface water in the Chios Basin (S = 38.4–38.8), with σ_t-values of 25.5 to 27.5 (Figure 7c). The $\Delta\Phi_{5/40}$ distribution illustrates the presence of relatively lighter water ($\Delta\Phi_{5/40} = 0.90$–0.95 m^2 s^{-2}) covering the Lemnos Plateau and the Thracian Sea, with the core of the BSW plume located at the south-west end of Samothraki Island, thus determining the anticyclonic baroclinic circulation of the surface layer (Figure 7d). Across the frontal zone, the geopotential anomaly $\Delta\Phi_{5/40}$ rapidly reduces to near zero values, while intermediate values (0.40–0.70 m^2 s^{-2}) are obtained in the mixing zones of the Sporades and Athos Basins.

A strongly stratified water column, induced by BSW expansion over the Thracian Sea, is shown in the meridian transect at 25°E (Figure 8). Temperature and salinity isolines depict a downward slope from the Lemnos Plateau towards the Thracian Sea continental shelf (1:3100 m or 0.02°), where the BSW achieves its maximum thickness, turning upwards nearer the coast, thus producing a prominent anticyclonic movement near Samothraki Island. Cold water at 13–14°C occupies the deeper parts of the coastal water columns, moving deeper (between 100 and 150 m) across the Thracian Sea shelf, towards the North Aegean Trough and Lemnos Plateau.

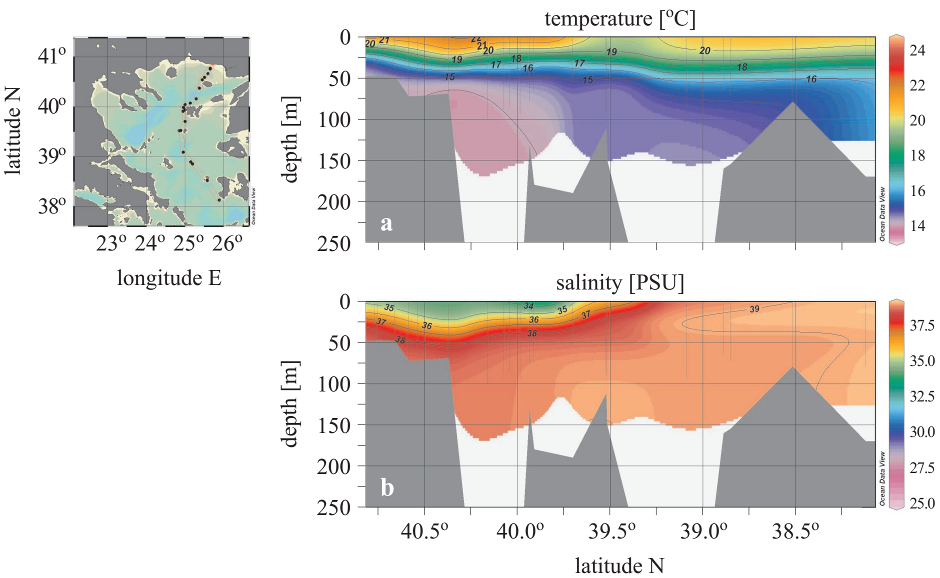

Figure 8. Distribution of water temperature (a) and salinity (b) along the 25°E meridian transect in summer 2000

3.4. The 2001 cruise

The results from this cruise reveal significant changes in the distribution of North Aegean Sea water masses, especially in terms of BSW salinity, as compared to those observed during the 1998–2000 summer periods. Strong surface temperature gradients prevail in the east-west direction, with relatively cooler water of 19.20–21.20°C around Lemnos and Lesvos Islands, and warmer conditions of 25.00–26.70°C along the north-western coastline (the Halkidiki Peninsula and Strymonikos Gulf). Such a temperature distribution induces the presence of a north-to-south oriented thermal frontal zone, crossing the Athos Basin and relaxing over the Sporades and Chios Basins (Figure 9a). An increased BSW salinity (34.0–34.7) is recorded during this cruise over the Thracian Sea and partly over the Lemnos Plateau (Figure 9b). A limited BSW core ($S = 31.15$, in the first 2 m depth) is detected along the southern coastline of Lemnos Island, while the LIW convergence zone appears displaced (following a sigmoidal track) to the north-west of Lemnos. LIW ($T = 21.5$–22.1°C; $S = 38.2$–38.8; $\sigma_t = 26.2$–

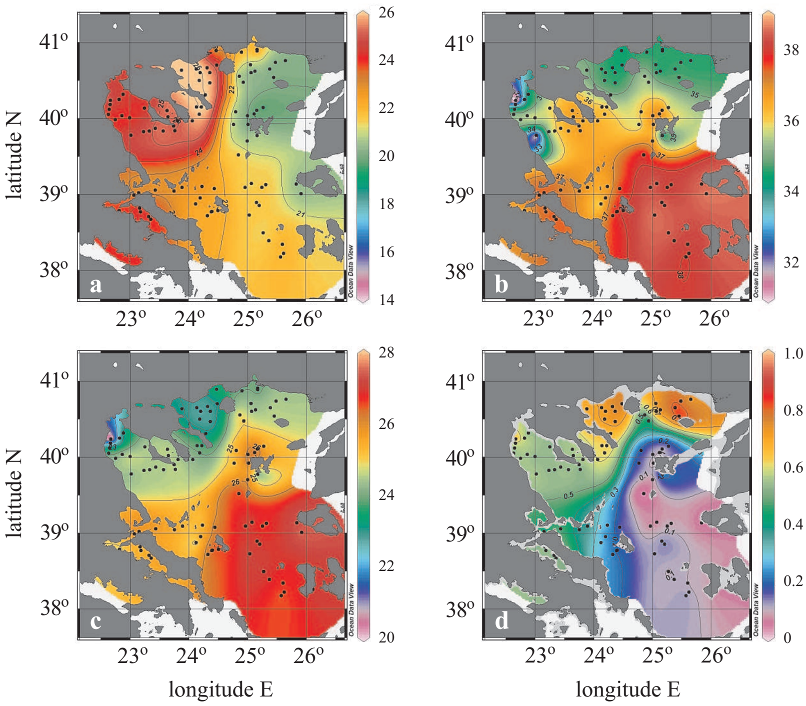

Figure 9. Horizontal distribution of water temperature (a), salinity (b), density σ_t (c) and geopotential anomaly ($\Delta\Phi_{0/40\,\mathrm{m}}$) (d) at the surface of the North Aegean Sea in summer 2001

27.4) propagates northwards as far as 39.5°N, while the less saline BSW covers the whole Thracian Sea and expands westwards into Strymonikos Gulf. In Thermaikos Gulf, freshwater plumes ($T = 23.8$–24.3°C; $S = 15$–30) are developed moving southwards along the mainland coast, but this water seems insufficient to reach the Sporades Basin surface layer, which appears supplied by the rapidly mixed BSW (Figure 9c). The horizontal geopotential anomaly ($\Delta\Phi_{5/40}$) gradient clearly displays a northward propagation in the BSW-LIW convergence zone between Imvros and Thassos Islands, the lighter BSW core at the north-west end of Samothraki Island (0.90–1.02 m^2 s^{-2}), and the intermediate $\Delta\Phi$-values in Thermaikos Gulf (0.4–0.6 m^2 s^{-2}) (Figure 9d). The 25°E meridian transect illustrates the changes in the water column dynamics (Figure 10). Thermal stratification in the Thracian Sea appears weak ($\Delta T = 4.2$°C), with the thermocline being lowered between 25 and 40 m. The lighter BSW appears to be suppressed

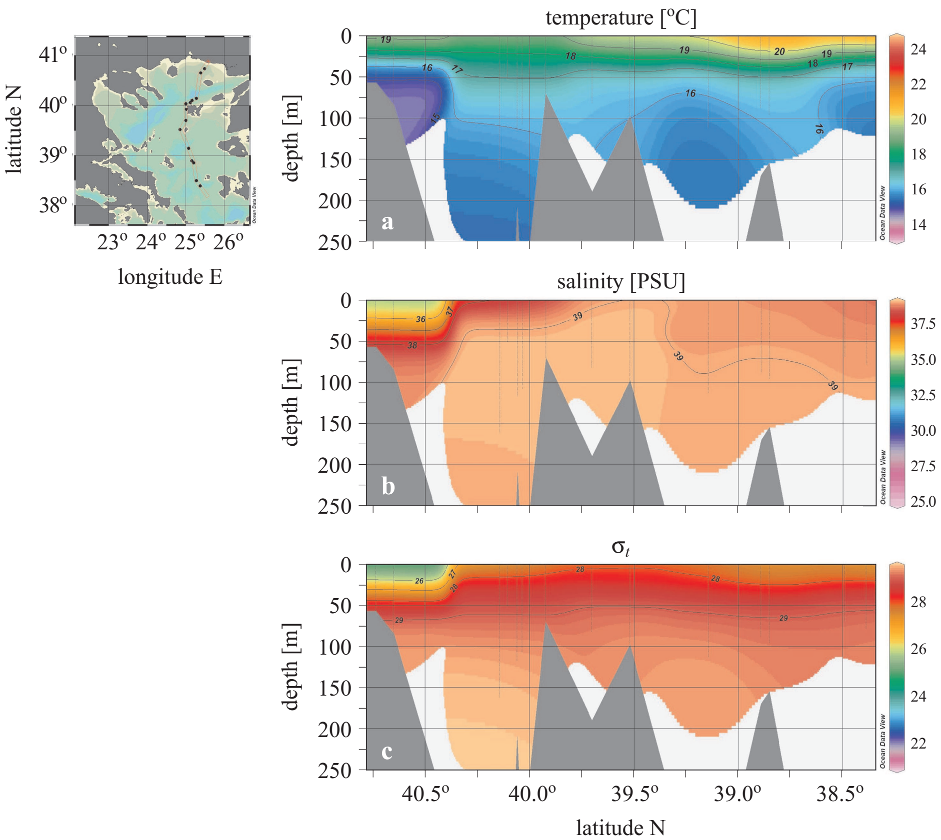

Figure 10. Distribution of water temperature (a), salinity (b) and density σ_t (c), along the 25°E meridian transect in summer 2001

between the Thracian Sea coastline and the outer zone of the Samothraki Plateau.

4. Discussion

4.1. Meteorological impact on SST and stratification

Water circulation, and water mass characteristics and distribution at the surface layer of the North Aegean Sea depend strongly on the buoyancy inflow of waters of Black Sea origin through the Dardanelles Straits, inducing the development and evolution of a freshwater plume. Superimposed on this regime lies the impact of air-sea heat exchanges along with the influence of the prevailing wind shear stresses. As these factors exhibit significant seasonal and interannual variability, corresponding changes are expected in the surface circulation, in the strength and the position of eddies and frontal zones, and in the water column dynamics of the North Aegean Sea (Zodiatis et al. 1996, Poulos et al. 1997). Moreover, surface temperature and salinity trends in the North Aegean Sea, attributed to variations in the heat, water and salt budgets of the area, may cause changes in the intermediate and deep water mass characteristics (Bethoux & Gentili 1999). Ginzburg et al. (2004) associated the Black Sea interannual surface temperature variability with ENSO events, showing the occurrence of a warmer summer during 1998 (associated with an 'El Niño' event during February 1997 to April 1998) and a warm winter and summer during 1999 (associated with a 'La Niña' event between May 1998 and December 2000). Similar relations were also reported by Kazmin et al. (2010), showing a gradual SST increase in the Black Sea between 1994 to 1999, in connection with local and large-scale atmospheric forcing, and a lagged North Aegean SST behaviour.

Indeed, the 1998–2001 North Aegean Sea surface data, averaged spatially over the main physiographic units (Table 2), suggest the occurrence of significantly warmer surface water masses over the Thracian Sea and Lemnos Plateau during the summers of 1999 (24.07°C and 22.66°C, respectively) and 2000 (22.67°C and 22.58°C, respectively). Similar patterns were depicted in the Sporades Basin, with warmer water observed during the summers of 1999 (24.48°C) and 2000 (25.02°C), probably attributed to the advection of warmer BSW combined with local heat exchange and mixing processes. In contrast, surface water variability in the LIW-dominated Chios Basin showed a gradual temperature decrease, from 23.36°C in 1998 to 21.52°C in 2001. Increased surface water temperature in the Thracian Sea, Lemnos Plateau and Sporades Basin seems counterbalanced by relatively cooler subsurface water of 13.98°C, 14.11°C and 13.84°C, respectively, during the summer 2000 period.

Table 2. Summary data for North Aegean Sea layers

	Thracian Sea			Limnos Plateau			Chios Basin			Sporades Basin		
	T[°C]	S	σ_t	T[°C]	S	σ_t	T[°C]	S	σ_t	T[°C]	S	σ_t
1998												
surface	20.45	34.00	23.89	21.95	31.57	21.63	23.36	38.35	26.38	24.32	36.01	24.32
mean 0–50 m	15.93	36.50	27.00	16.96	36.92	27.09	18.28	38.82	28.21	17.02	37.77	27.71
mean 50–200 m	14.04	38.63	29.41	14.22	38.85	29.55	15.05	39.03	29.51	13.94	38.63	29.45
1999												
surface	24.07	32.38	21.65	22.66	33.17	22.65	22.83	39.00	27.03	24.48	36.79	24.86
mean 0–50 m	16.64	37.84	27.83	17.27	38.13	27.91	17.41	39.05	28.58	14.98	38.52	28.51
mean 50–200 m												
2000												
surface	22.67	34.10	23.36	22.58	32.94	22.50	21.30	38.62	27.18	25.02	35.57	23.77
mean 0–50 m	17.78	36.49	26.54	18.13	36.68	26.62	18.62	39.08	28.34	18.54	37.85	27.38
mean 50–200 m	13.98	38.83	29.52	14.11	38.85	29.51	15.53	39.16	29.41	13.84	38.74	29.48
2001												
surface	20.54	34.78	24.45	20.33	36.33	25.70	21.52	38.44	26.98	22.34	36.94	25.61
mean 0–50 m	17.33	36.59	26.73	17.83	38.68	28.24	18.68	38.84	28.14	18.51	38.41	27.85
mean 50–200 m	14.53	38.80	29.43	15.53	39.04	29.37	15.50	39.01	29.37	15.10	38.91	29.35

Furthermore, during these warmer winter and summer periods over the broader Black Sea area, evaporation and subsequent precipitation rates increase, and since the system functions under a positive water balance (Özsoy & Ünlüata 1997), this may increase the BSW outflow through the Dardanelles, stabilizing thermal and saline water column stratification (Stanev & Peneva 2002). Present results indicate a strongly stratified water column throughout the Thracian Sea ($\Delta T_{0/50\,\mathrm{m}} = 9.20°\mathrm{C}$; $\Delta S_{0/50\,\mathrm{m}} = 6.8$) and the Lemnos Plateau ($\Delta T_{0/50\,\mathrm{m}} = 7.60°\mathrm{C}$; $\Delta S_{0/50\,\mathrm{m}} = 6.1$) during summer 1999. The influence of southerly winds in summer 2001 promoted turbulent mixing ($\Delta S_{0/50\,\mathrm{m}} = 2.7$), leading to the elevated surface salinity values recorded in the Thracian Sea (34.78), Lemnos Basin (36.33) and Sporades Basin (36.94), followed by a lowering of the halocline down to 70 m depth. Wind mixing gradually shifts the bottom of the BSW layer to warmer and

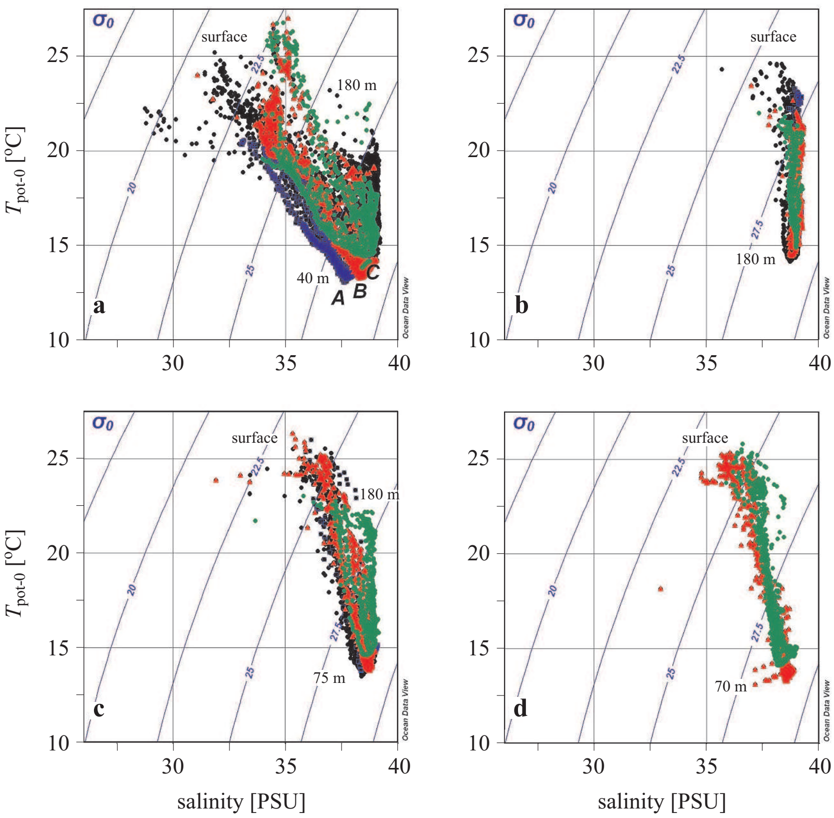

Figure 11. Temporal variability of water mass characteristics in the Thracian Sea and Lemnos Plateau (a), Chios Basin (b), Sporades Basin (c) and Thermaikos Gulf (d); (black squares: 1998; blue squares: 1999; red triangles: 2000; green circles: 2001)

more saline conditions. This is shown in Figure 11a, which presents the T-S diagram for the Thracian Sea and Lemnos Plateau. Point A ($T = 13.14°$C, $S = 37.57$, $\sigma_t = 28.52$) defines the bottom of BSW in summer 1999, point B in summer 2000 ($T = 13.31°$C, $S = 38.35$, $\sigma_t = 29.16$) and point C during summer 2001 ($T = 14.39°$C, $S = 38.58$, $\sigma_t = 29.10$). Similar effects of turbulent mixing appear in the Sporades Basin (Figure 11c) and Thermaikos Gulf (Figure 11d), while in the Chios Basin the thermohaline conditions remain almost unchanged (Figure 11b).

The influence of turbulent mixing and horizontal LIW transport under local southerly winds may only partially explain the increased salinity values observed at the surface of the Thracian Sea and Lemnos Plateau in summer 2001. Another important mechanism appears to be the turbulent mixing taking place along the so-called Turkish Straits (TS) conduit (consisting of the Sea of Marmara, the Straits of Istanbul and the Dardanelles), thus increasing the total salt content of BSW outflow in the North Aegean Sea. Indeed, during the late May–early June 2001 period, strong south-westerly gales prevailed along the TS, rapidly changing to vigorous north-easterly Etesians. Under south-westerly winds, the denser North Aegean Sea water increases its thickness along the Dardanelles, supporting vertical mixing and promoting salt diffusion to the upper layer, thus returning salt back to the Mediterranean (Yüce 1996, Özsoy & Ünlüata 1997, Stashchuk & Hutter 2001). In contrast, north-easterly winds, dominant during the 1998, 1999 and 2000 summer sampling periods, cause southward surface currents to increase and northward bottom currents to decrease (Yüce 1996). Under these conditions, the thickness of Mediterranean water decreases and vertical mixing is limited as a result.

4.2. Response of BSW-LIW front and Samothraki Anticyclone to wind forcing

At the sub-basin scale field of gyres and flows, the BSW-LIW frontal zone and the Samothraki Anticyclone appear as the most prominent surface features of the North Aegean Sea. Horizontal density gradients across the frontal interface appear stronger during the 1998 conditions ($\Delta\sigma_t =$ 0.11 per km), reducing to 0.05 per km in 2001, due to horizontal and vertical mixing induced by southerly winds. A significant cross-frontal horizontal geopotential anomaly gradient ($\Delta\Phi_{5/40} = 0.012$–$0.018$ m^2 s^{-2} per km) remains almost constant throughout the samplings. The Samothraki Anticyclone appears as a permanent feature in the area, containing a low density core (supplied by the less saline BSW) that produces both an upward doming of the sea surface, detectable by satellite altimeters (Larnicol et al. 2002), and a strong clockwise geostrophic circulation (Theocharis & Georgopoulos 1993). The horizontal distribution of the geopotential anomaly (contour of $\Delta\Phi_{0/40} > 0.8$ m^2 s^{-2}) was used to identify the anticyclone's core water. It occurred that in summers 1998 and 2000, under northerly winds, the anticyclone was located to the north-west of Lemnos Island (Figure 4d) and to the south-west of Samothraki Island (Figure 7d) respectively, while in summer 2001, under the influence of strong south to south-westerly winds, it moved to the north-west of Samothraki Island (Figure 9d). Figure 12 illustrates the eastward/westward baroclinic transport in the 0/40 m layer along the 25°E meridian. It turns out that in summers 1998–2000, under the influence of northerly winds, the Samothraki Anticyclone achieved almost symmetrical forms in terms of eastward/westward surface layer transport. Moreover, westward baroclinic transport induced by the BSW outflow was observed in deep water. In summer 2001, as the Samothraki Anticyclone moves northwards, it seems to collide on the Thracian Sea continental slope and then interact with the westward spreading Evros river plume, thus reducing the anticyclone's eastward moving branch, while the westward transport appears intensified. Shi & Nof (1993) showed that such collision ultimately leads to the eddy splitting into two with opposing signs. Further south, it turns out that

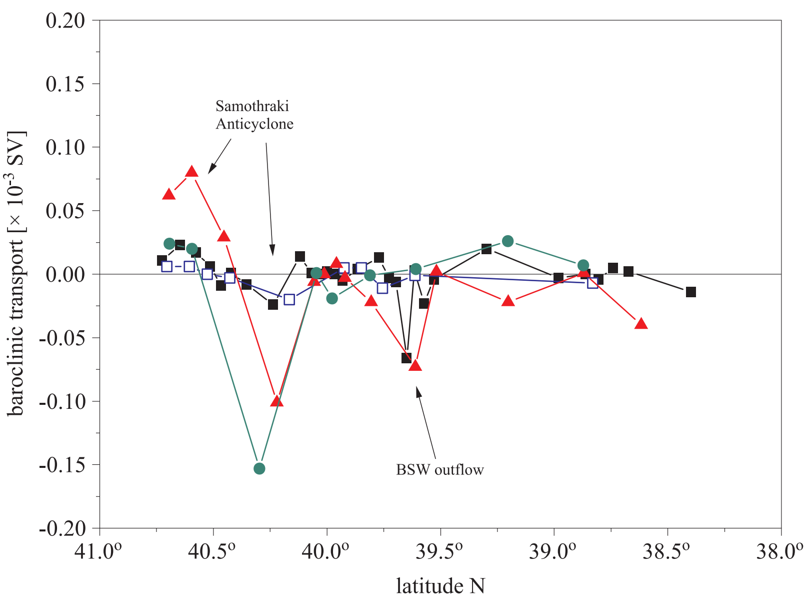

Figure 12. Baroclinic transport in the surface 0/40 m layer (positive – eastward; negative – westward) along the 25°E meridian transect; (black squares: 1998; blue squares: 1999; red triangles: 2000; green circles: 2001)

the sharp increase in the salt content of the BSW layer in summer 2001 produced limited west-orientated baroclinic currents (Figure 12).

Considering these findings to be typical of the impact of the wind shear stress on the behaviour of sub-basin scale patterns in the North Aegean Sea, one may argue that strong southerly winds tend to displace the BSW-LIW frontal zone to the north of Lemnos Island, thus suppressing the anticyclone towards the Thracian Sea continental shelf. Under these conditions the system reduces its radius and deepens, increasing its surface elevation at the centre, leading to surface convergence and subsurface divergence associated with the halocline lowering due to downwelling effects. On the other hand, northerly winds tend to return the BSW-LIW front to its regular position (south of Lemnos Island), allowing the horizontal expansion of the Samothraki Anticyclone. Gyre horizontal expansion favours surface slope reduction, leading to surface divergence and subsurface convergence, thus allowing isopycnals to gradually rebound towards the surface, causing upwelling. As low-density water in the upper part of the anticyclone moves radially outwards, it is replaced by deeper water moving upwards from the core of the eddy, which in turn is replaced by denser deep water moving radially inwards from the eddy margins. This mechanism has been suggested by several investigators (Pinot et al. 1995, Mackas et al. 2005).

Strong winds from alternate north-to-south directions, lasting for a few days over the Aegean Sea, may cause such Samothraki Anticyclone suppression/expansion events, resulting in significant vertical movements within the system. These water movements could be responsible for the occurrence of lenses with cooler and saline (upwelled) or fresher and warmer (downwelled) water observed regularly in the water column (between 10–30 m depth) over the Thracian Sea continental shelf (Zervakis & Georgopoulos 2002). As the wind rapidly changes its orientation during the winter (Poulos et al. 1997), this mechanism could also support the occurrence of surface saline 'tongues', leading ultimately to deep water formation events along the Thracian Sea continental shelf, as reported by Theocharis & Georgopoulos (1993).

A quantitative estimation of vertical velocity could be obtained following the quasi-geostrophic density equation procedure (Pinot et al. 1995):

$$\frac{\partial \rho}{\partial t} + u_g \frac{\partial \rho}{\partial x} + v_g \frac{\partial \rho}{\partial y} + w \frac{\partial \rho}{\partial z} = 0, \tag{1}$$

which gives

$$w = w_x + w_y + w_t = -\alpha_x u_g - \alpha_y v_g + w_t, \tag{2}$$

where

$$\alpha_x = \frac{\partial\rho/\partial x}{\partial\rho/\partial z}, \ \alpha_y = \frac{\partial\rho/\partial y}{\partial\rho/\partial z}, \ \text{and} \ w_t = -\frac{\partial\rho/\partial t}{\partial\rho/\partial z}. \tag{3}$$

Following the determination of eastward/westward baroclinic transport in the 0/40 m layer along the 25°E meridian transect, α_y can be estimated from the elevation of isopycnals of $\Delta z = 1$ m over a distance of $\Delta y = 2500$ m, for 1998. Since $w_y/v_g = \alpha_y = \Delta z/\Delta y$, by taking $v_g = 0.1$ m s^{-1}, one obtains a vertical velocity $w_y = 4 \times 10^{-5}$ m s^{-1}. Similarly, for the 2001 distribution, with a limited geostrophic velocity $v_g = 0.05$ m s^{-1} and an isopycnal elevation of $\Delta z = 17$ m over a distance of $\Delta y = 56\,000$ m, a reduced vertical velocity of $w_y = 1.5 \times 10^{-5}$ m s^{-1} is induced.

Indeed, relative vertical velocity estimations using the above described quasi-geostrophic density equation appear to be in accordance with chlorophyll *a* concentration time series, recorded using SeaWiFS over the Samothraki and Lemnos Plateaus (Groom et al. 2006). The results show that the Samothraki Anticyclone could sustain the presence of increased chlorophyll *a* concentrations (3–5 mg m^{-3}) in summer 1998 and 1999, when vertical velocity values were higher, as opposed to the lower chlorophyll *a* concentrations (0.7–1.0 mg m^{-3}) in summer 2001, under lower convective movement conditions.

5. Conclusions

The variability of surface water masses in the North Aegean Sea was studied utilizing a series of 360 CTD profiles obtained during the summers of 1998–2001. The results depicted the temporal variability of the Black Sea Water (BSW) plume expansion, changes in the characteristics of the BSW-LIW frontal zone, and variations in the location and radius of sub-basin scale hydrographic features (such as the Samothraki Anticyclone). The occurrence of significantly warmer surface water masses over the Thracian Sea and Lemnos Plateau in summer 1999 and 2000 suggested a dependence of North Aegean Sea surface dynamics on Black Sea freshwater inputs and global atmospheric forcing (as ENSO events). Furthermore, the results demonstrated the presence of water of relatively higher salinity at the surface of the Thracian Sea and Lemnos Plateau during the summer of 2001, attributed to strong turbulent wind mixing along the Turkish Straits and the local meteorological influence over the North Aegean Sea. Under the action of strong southerly winds, the horizontal density gradients across the BSW-LIW frontal zone appear relaxed and are displaced to the north of Lemnos Island, while under northerly wind stresses, the front returns to its regular position (south of Lemnos Island).

Finally, the present work indicated the importance of transient winds on the horizontal expansion/suppression events of the Samothraki Anticyclone, leading to significant convective movements within the system. Analysis of geostrophic currents along the 25° meridian transect showed that the horizontal baroclinic transport varied from 0.02 to 0.1 10^{-3} Sv, while approximations of the quasi-geostrophic density equation produced vertical convective movement estimates of 1.5–4 10^{-5} m s^{-1}.

Acknowledgements

The authors wish to thank Captain E. Maniatis and the crew of the fishing vessel 'Evagelistria' for their help during the sampling periods.

References

Bethoux J. P., Gentili B., 1999, *Functioning of the Mediterranean Sea: past and present changes related to freshwater input and climate changes*, J. Marine Syst., 20 (1–4), 33–47.

Cordero S. G., 1999, *The use of thermal satellite data in dense water formation studies in the Mediterranean Sea*, J. Marine Syst., 20 (1–4), 175–186.

Gertman I. F., Ovchinnikov I. M., Popov Yu. I., 1990, *Deep-water formation in the Aegean Sea*, CIESM Congr. Proc., 32 (1), 164 pp.

Ginzburg A. I., Kostianoy A. G., Sheremet N. A., 2004, *Seasonal and interannual variability of the Black Sea surface temperature, as revealed from satellite data (1982–2000)*, J. Marine Syst., 52 (1–4), 33–50.

Groom S., Shutler J., Mottram G., 2005, *Satellite data analysis for the North Aegean Sea*, [in:] *ANREC Project final report*, [EU contract No. QLRT-2001-01216 ANREC], 120–153.

Ivanov V. A., Kovalenko T. P., Nikolayenko Ye. G., 1989, *Structure and characteristics of fronts in the Mediterranean Sea in summer of 1986*, Oceanology, 29, 434–437.

Kazmin A., Zatsepin A. G., Kontoyiannis H., 2010, *Comparative analysis of the long-term variability of winter surface temperature in the Black and Aegean Seas during 1982–2004 associated with the large-scale atmospheric forcing*, Int. J. Climatol., 30 (9), 1349–1359.

Kontoyiannis H., Kourafalou V. H., Papadopoulos V., 2003, *Seasonal characteristics of the hydrology and circulation in the Northwest Aegean Sea (eastern Mediterranean): observations and modelling*, J. Geophys. Res., 108 (C9), 3302, doi:10.1029/2001JC001132.

Larnicol G., Ayoub N., Le Traon P. Y., 2002, *Major changes in Mediterranean Sea level variability from 7 years of TOPEX/Poseidon and ERS-1/2 data*, J. Marine Syst., 33–34, 63–89.

Lascaratos A., 1992, *Hydrology of the Aegean Sea*, [in:] *Winds and currents of the Mediterranean Basin*, H. Charnock (ed.), Rep. Meteorol. Oceanogr., Vol. 40, Harvard Univ., Stroudsberg, 313–334.

Latif M. A., Özsoy E., Oguz T., Ülüata Ü., 1991, *Observations of the Mediterranean inflow into the Black Sea*, Deep-Sea Res., 38 (Suppl. 2), 711–723.

Lykousis V., Chronis G., Tselepides A., Price N. B., Theocharis A., Siokou-Frangou I., van Wambeke F., Danovaro R., Stavrakakis S., Duineveld G., Georgopoulos D., Ignatiades L., Souvermezoglou A., Voutsinou-Taliadouri F., 2002, *Major outputs of the recent multidisciplinary biogeochemical researches undertaken in the Aegean Sea*, J. Marine Syst., 33–34, 313–334.

Mackas D. L., Tsurumi M., Galbraith M. D., Yelland D. R., 2005, *Zooplankton distribution and dynamics in a North Pacific Eddy of coastal origin: II. Mechanisms of eddy colonization by and retention of offshore species*, Deep-Sea Res. Pt. II, 52 (7–8), 1011–1035.

Oguz T., Sur H., 1989, *A two-layer model of water exchange through the Dardanelles Strait*, Oceanol. Acta, 12, 23–31.

Olson D. B., Kourafalou V. H., Johns W. E., Samuels G., Veneziani M., 2007, *Aegean surface circulation from a satellite-tracked drifter array*, J. Phys. Oceanogr., 37 (7), 1898–1917.

Ovchinnikov I. M., 1966, *Circulation in the surface and the intermediate layers of the Mediterranean*, Oceanology, 6, 48–58.

Özsoy E., Ünlüata Ü., 1997, *Oceanography of the Black Sea: a review of some recent results*, Earth-Sci. Rev., 42 (4), 231–272.

Pinot J.-M., Tintore J., Lopez-Jurado J. L., Fernandez de Puelles M. L., Jansa J., 1995, *Three-dimensional circulation of a mesoscale eddy/front system and its biological implications*, Oceanol. Acta, 18 (4), 389–400.

Poulos S. E., Drakopoulos P. G., Collins M. B., 1997, *Seasonal variability in sea surface oceanographic conditions in the Aegean Sea (Eastern Mediterranean): an overview*, J. Marine Syst., 13 (1–4), 225–244.

Schlitzer R., 2005, *Ocean data view*, http://www.awi-bremerhaven.de/GEO/ODV.

Sempéré R., Panagiotopoulos C., Lafont R., Marroni B., van Wambeke F., 2002, *Total organic carbon dynamics in the Aegean Sea*, J. Marine Syst., 33–34, 355–364.

Shi C., Nof D., 1993, *The splitting of eddies along boundaries*, J. Mar. Res., 51 (4), 771–795.

Siokou-Frangou I., Bianchi M., Christaki U., Christou E. D., Giannakourou A., Gotsis O., Ignatiades L., Pagou K., Pitta P., Psara S., Souvermezoglou E., van Wambeke F., Zervakis V., 2002, *Carbon flow in the planktonic food-web along a gradient of oligotrophy in the Aegean Sea (Mediterranean Sea)*, J. Marine Syst., 33–34, 335–353.

Stanev E. V., Peneva E. L., 2002, *Regional sea level response to global climate change: Black Sea examples*, Global Planet. Change, 32 (1), 33–47.

Stashchuk N., Hutter K., 2001, *Modelling of water exchange through the Strait of the Dardanelles*, Cont. Shelf Res., 21 (13–14), 1361–1382.

Theocharis A., Georgopoulos D., 1993, *Dense water formation over the Samothraki and Limnos Plateaux in the north Aegean Sea (Eastern Mediterranean Sea)*, Cont. Shelf Res., 13 (8–9), 919–939.

Ünlüata Ü., Oguz T., Latif M. A., Özsoy E., 1990, *On the physical oceanography of Turkish Straits*, [in:] *The physical oceanography of sea straits*, L. J. Pratt (ed.), Kluwer Acad. Publ., Dordrecht, 25–60.

Velaoras D., Laskaratos A., 2005, *Deep water mass characteristics and interannual variability in the North and Central Aegean Sea*, J. Marine Syst., 53 (1–4), 59–85.

Vlasenko V. I., Stashchuk N. N., Ivanov V. A., Nikolaenko E. G., Uslu O., Benli H., 1996, *Influence of the water exchange through Dardanelles on the thermohaline structure of the Aegean Sea*, Bull. Inst. Océanogr. Monaco, Spec. No. 17, 147 –165.

Yüce H., 1995, *Northern Aegean water masses*, Estuar. Coast. Shelf Sci., 41 (3), 325–343.

Yüce H., 1996, *On the variability of Mediterranean water flow into the Black Sea*, Cont. Shelf Res., 16 (11), 1399–1413.

Zervakis V., Georgopoulos D., 2002, *Hydrology and circulation in the North Aegean (eastern Mediterranean) throughout 1997 and 1998*, Mediterr. Marine Sci., 3 (1), 7–21.

Zervakis V., Georgopoulos D., Drakopoulos P. G., 2000, *The role of the North Aegean in triggering the recent Eastern Mediterranean climatic changes*, J. Geophys. Res., 105 (C11), 26103–26116.

Zervakis V., Karageorgis A. P., Kontoyiannis H., Papadopoulos V., Lykousis V., 2005, *Hydrology, circulation and distribution of particulate matter in Thermaikos Gulf (NW Aegean Sea), during September 2001–October 2001 and February 2002*, Cont. Shelf Res., 25 (19–20), 2332–2349.

Zervakis V., Krasakopoulou E., Georgopoulos D., Souvermezoglou E., 2003, *Vertical diffusion and oxygen consumption during stagnation periods in the deep North Aegean*, Deep-Sea Res. Pt. I, 50 (1), 53–71.

Zodiatis G., 1994, *Advection of the Black Sea Water in the North Aegean Sea*, Global Atmos. Ocean. Syst., 2 (1), 41–60.

Zodiatis G., Alexandri S., Pavlakis P., Jonsson L., Kallos G., Demetropoulos A., Georgiou G., Theodorou A., Balopoulos E., 1996, *Tentative study of flow patterns in the North Aegean Sea using NOAA-AVHRR images and 2D model simulation*, Ann. Geophys., 14 (11), 1221–1231.